THE EVOLUTION AND APPLICATION OF ASYMMETRICAL IMAGE FILTERS FOR QUANTITATIVE XCT ANALYSIS

N. L. Rupert[1], J. M. Wells[2], W. Bruchey[3], and J. R. Wheeler[4]

[1]*KLNG Enterprises, 122 Bradish Road, Kittanning, PA 16201-4306, USA, email: nevinlr@comcast.net*
[2] *JMW Associates, 102 Pine Hill Blvd., Mashpee, MA 02649-2869, USA, email: jmwconsultant@comcast.net*
[3]*Service Engineering Corporation4695 Millennium Dr, Belcamp, MD 21017-1505, USA, email: wbruch@hughes.net*
[4]*Marshall University – Huntington, WV 25755, USA, email: jeffw@xrayct.com*

The successful use of nondestructive x-ray computed tomography (XCT) techniques to characterize and visualize ballistic impact damage has been demonstrated. Their high resolution two-dimensional (2-D) tomographic slices and three-dimensional (3-D) virtual solid object reconstructions represent a telling, spatially accurate, and qualitatively informative rendering of the internal damage present. However, the damage is not presented in a format that allows the XCT damage reconstructions to be directly compared with hydrocode modeling of the same ballistic event. An initial attempt to bridge the difference between the two diagnostic techniques was made by converting the XCT data into damage fractions as a function of depth and radius (from the impact center), assuming an axial-symmetrical damage profile. The next step addressed the automation of the conversion process. In this paper, the authors address the conversion of XCT impact damage data into true 3-D damage fractions as a function of depth, radius, and rotational angle. This data conversion more closely describes the asymmetrical damage observed in the 2-D tomographic slices and 3-D virtual solid reconstructions, and the type of information required for future validation of full 3-D hydrocode damage modeling.

BACKGROUND

The successful use of nondestructive x-ray computed tomography (XCT) techniques to characterize and visualize ballistic impact damage has been demonstrated. Examples of some of the dramatic visualizations of impact damage details previously unobserved and/or uncharacterized before the introduction of evolving XCT damage diagnostic techniques are shown in Figure 1.[1-7] Included are observations of segmented (virtually isolated) penetrator fragments, novel cracking morphologies including three-dimensional (3-D) superimposed hourglass-shaped ring cracks and spiral cracking, 3-D quantification and spatial mapping of damage fraction levels, impact-induced porosity, impact surface topological radial cracking, and near-surface radial expansion and surface debris. However, the damage is not presented in a format that allows the XCT damage reconstructions to be directly compared with hydrocode modeling of the same ballistic event.

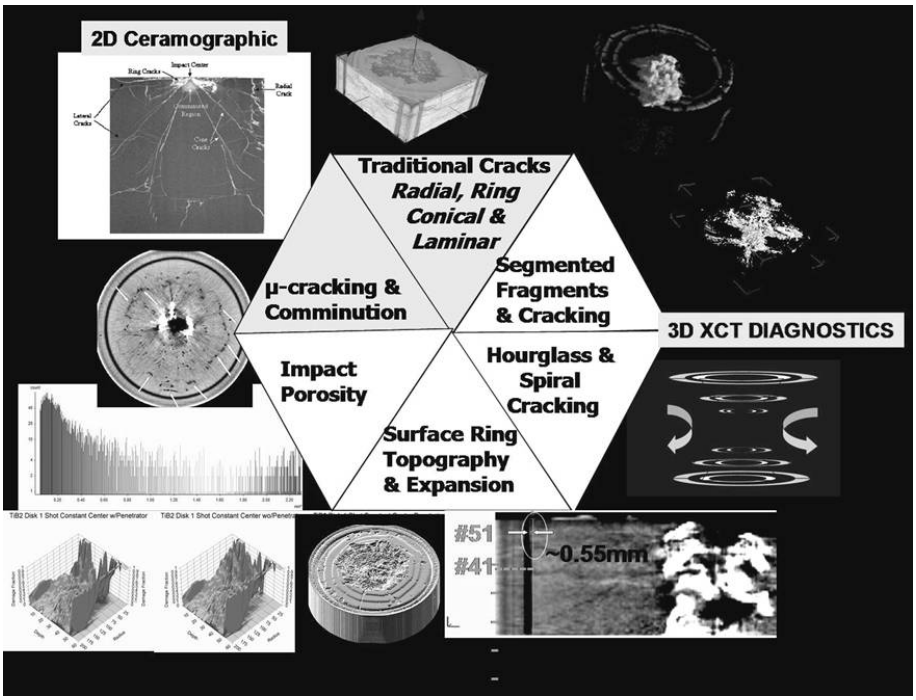

Figure 1. Examples of ballistic impact damage details and morpholgies including those traditionally observed and those characterized with XCT damage diagnostic techniques.

An initial attempt to bridge the difference between the two diagnostic techniques was made by converting the XCT data into damage fractions as a function of depth and radius (from the impact center), assuming an axial-symmetrical damage profile.[6] The second step addressed the automation of the conversion process for the axial-

symmetrical problem.[7-8] In this paper, the authors address the conversion of XCT impact damage data into true 3-D damage fractions as a function of depth and position. This type of information is required for future validation and verification of full 3-D hydrocode damage modeling.

DESIGN A FILTER

Arbitrary Filter Limitations

The ratios of the voxel dimensions must be considered in determining an appropriate sample volume size. The scan/voxel thickness is set as the basic unit of length in determining an appropriate sample volume size in this study. The total height and width of the voxels used in the sampling technique need to be between 1/3 and 3× the voxel thickness to avoid geometrically skewing the results. For this study, the height and width of a single voxel is assumed to be 1/3 the voxel thickness. Next, the height and width of the sample must correspond to an odd number of voxels to prevent a shift in the position registration for the filtered data in relation to the original binarized XCT data. Finally, only two types of sampling patterns were considered at this time, the square (S) and diamond (D) listed in Table 1 and illustrated in Figure 2.

Table 1. Sample filters.

Filter Sample Pattern Designation	Number of Voxels in Sample Pattern	Maximum Rate of Change in Unit Damage Fraction Possible		Number of Unit Damage Levels Possible
		Along Axis	45° Diagonal	
S-1	1	1.00	1.00	2
D-3	5	0.60	0.60	6
S-3	9	0.33	0.56	10
D-5	13	0.38	0.38	14
S-5	25	0.20	0.36	26
D-7	25	0.28	0.28	26
S-7	49	0.14	0.27	50
D-9	41	0.22	0.22	42
S-9	81	0.11	0.21	82

Table 1 lists a rough comparison of number of unit damage levels and maximum rate of change inherent for each of the patterns. Initial application of these filter patterns for generating a unit damage fraction (mathematical representation of the fraction of damaged material within a given volume of space) assumes a uniform weighing of each voxel contribution.

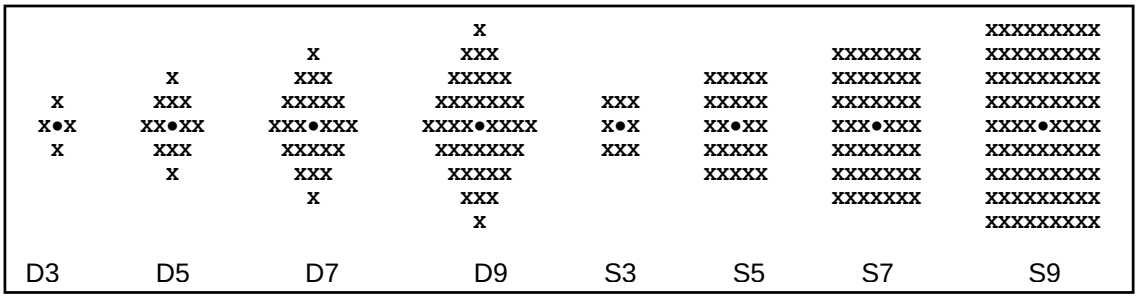

Figure 2. Sample filter patterns.

Test Patterns for Evaluation

A series of test patterns representing binarized XCT data were generated to evaluate the proposed filters, as illustrated in Figure 3. In this illustration, the X- and Y-coordinates show position registration on a given axial slice plane. The Z-axis represents the unit damage fraction, where 0 is undamaged, and 1 is fully damaged. These patterns represent an edge, an outside corner, an inside corner, a 1-voxel-wide single crack, a standard-unit-wide single crack (3 voxels wide), a single wide crack (9 voxels wide), and multiple cracks with increasing spacing between cracks. The contrast between filters D7 and S5 should approximate the effects of a 45° obliquity crack with the two filter baseline geometric schemes, thereby reducing the number of test cases for this initial screening.

CURSORY APPLICATION AND ANALYSIS OF FILTERS

The application of filters is based on the reasonable assumption that the physical variations in density as measured by XCT analysis correlate with the virtual mathematical simplification in the use of unit damage fraction to describe a material's residual properties when partially damaged. The process of converting to a damage fraction estimate is a three-step process. First, an XCT reconstructed image made up of voxels that are an integer value proportional to the average linear attenuation coefficient of the material is obtained. This linear attenuation coefficient is approximately proportional to the physical density of the material and is a function of the effective atomic number of the material and the spectral distribution of the x-ray beam. The voxel values are sometimes referred to as density or x-ray density values, and they are useful when interpreting individual images. However, other factors (including beam hardening, edge artifacts, and partial-volume artifacts) effect this value when objects contain multiple materials or when images obtained at different energies

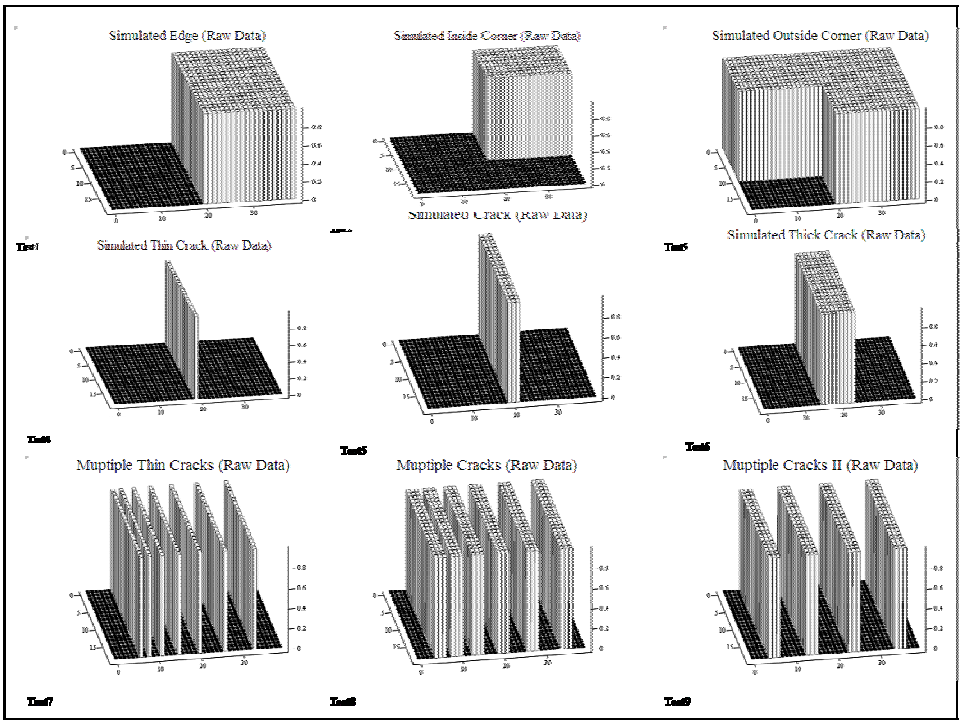

Figure 3. Binary test patterns.

prevent their direct conversion into an estimation of the unit damage fraction.[9] The second step is the normalization or binarization of the XCT image. The image is passed through a filter that converts the individual linear attenuation coefficients into a 1 or 0, based on an arbitrary threshold value. This threshold value is normally set at the midpoint value between the maximum and minimum linear attenuation coefficients within the XCT reconstructed image of the material of interest. The third and final step is the application of a second filter to synthetically create the unit damage fraction based on adjacent voxel values after binarization of the image (illustrated in Figure 4).

Damage features present in the raw binary data increasingly became obscured with the increase in filter sample size. This was especially true for damage smaller than the scan thickness. As a result, a weighting function was applied to the D3 and S3 filters later in the study. The weighting function assumed that the central voxel contributed 50% of the unit damage fraction, and the remaining voxels equally contributed to the remaining 50% of the unit damage fraction. This application of weighting function maintained some to the one-dimensional damage features illustrated in Figure 5. This figure shows how the equally weighted voxels in the S3 filter shift the apparent crack location with two closely spaced cracks, combine the damage from two

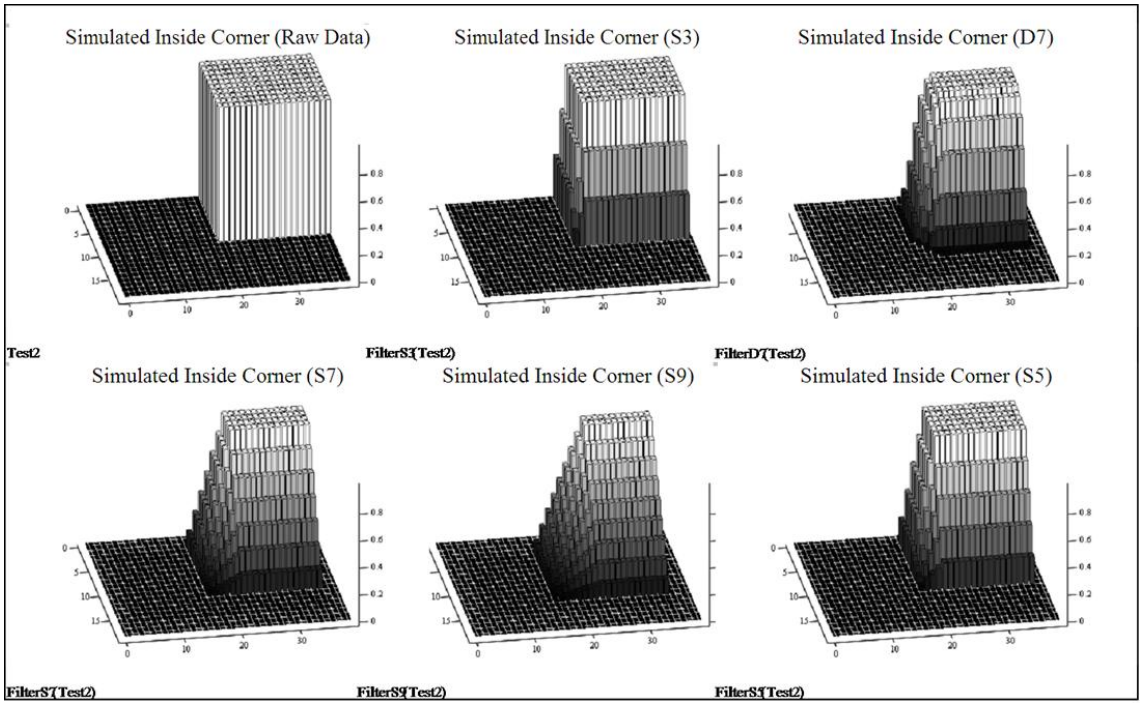

Figure 4. Comparison based on filter sample size.

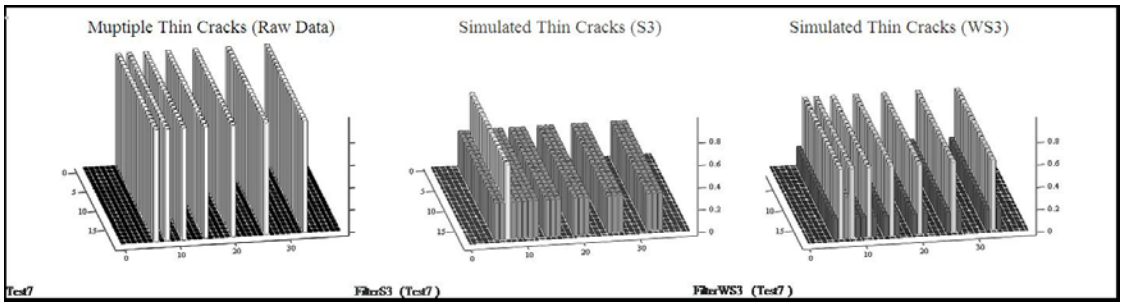

Figure 5. Multiple thin cracks with increasing space between cracks—(a) raw data, (b) S3 filter, and (c) weighted S3 filter.

cracks into a single damage area with a slight increase in spacing, and evolve into a filter with low-level damage areas instead of the individual cracks from the raw data. The addition of the simple voxel weighing function maintained the positioning of the subfilter-size cracks with a minimum of spread of the data and reduction in the unit

damage fraction. Figure 6 illustrates the negligible smearing of the two-dimensional damage features resulting from applying the weighting function to the filters.

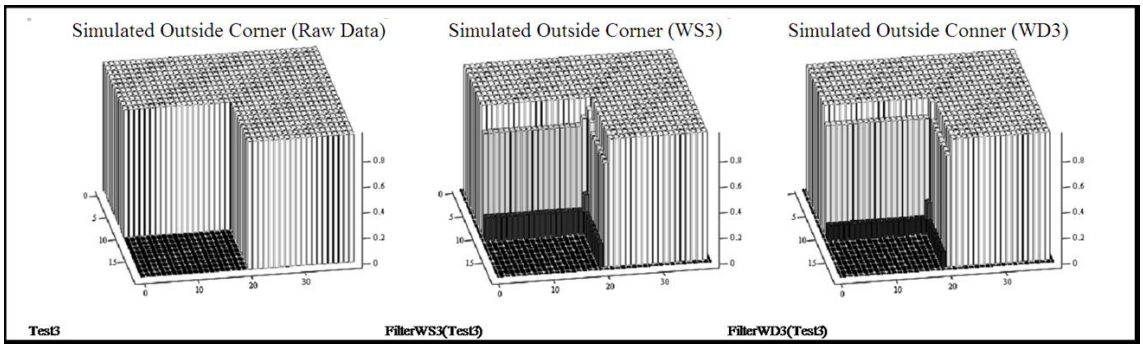

Figure 6. Inside corner comparison of (a) raw data, (b) weighted S3 filter, and (c) weighted D3 filter.

INTUITIVE BASED FILTER RECOMMENDATION

Because this is our initial approach at generating asymmetrical image filters for quantitative XCT analysis, the physical basis for quantitative verification of the generated unit damage fractions as a function of position have not been developed to date. The XCT analysis has improved our understanding of the several types of damage occurring and resulting from ballistic impact; however, its output does not directly bridge the binary physical world of damaged and undamaged physical states that can be measured to the virtual world of unit damage fractions generated by the computer modelers. The authors feel that XCT analysis, with the development of the proper filters, is the bridge between the physical and virtual worlds in penetration mechanics. As such, we recommend the following as the next small steps toward developing asymmetrical image filters:

1. The height and width of a single voxel should be set at ~1/3 the voxel thickness to help minimize geometric distortion.
2. The filter sampling should be approximately cubic in nature to minimize the geometric distortion and smearing of damage features detected by the binary XCT data.
3. A weighting function needs to be applied to the voxels within the filter sample to keep from suppressing or eliminating the subsample damage features within the filtered data set. This will also increase the number discernable unit damage fractions available as output from the filter.

4. The height and width of the sample must correspond to an odd number of voxels to prevent a shift in the position registration for the filtered data in relation to the original binarized XCT data. This will allow data to be converted to any coordinate system without losing precision.
5. In the binarization of the raw XCT data, a systematic application of multiple threshold values should be used and related via a weighting function to determine the unit damage fraction. This can potentially increase the accuracy of the measurement of unit damage fraction without increasing the sample size or obstructing the detection of damage features.
6. Once the binarized XCT data has been transformed into unit damage fractions, converting to a true asymmetrical representation of the data is a simple matter of coordinated transformation of the XCT slice coordinate registration. The Fast Fourier Transforms application can then be used to interpolate between registration points and smooth the surface features of the unit damage fraction data plots, thereby producing an output analogous to that provided by hydrocode modeling.

REFERENCES

[1] J. M. Wells, N. L. Rupert, W. H. Green, Progress in the 3-D Visualization of Interior Ballistic Damage in Armor Ceramics, *Ceramic Armor Materials by Design*, Eds. J. W. McCauley et al., Ceramic Transactions, **134**, 441-448 (2002)
[2] N. L. Rupert, J. M. Wells, W. H. Green, K. J. Doherty, Damage Assessment in TiB2 Ceramic Armor Targets, ARL-TR-2607, U.S. Army Research Laboratory: Aberdeen Proving Ground, MD (2001)
[3] J.M. Wells, On the Role of Impact Damage in Armor Ceramic Performance, *Proceedings of the 30th International Conference on Advanced Ceramics and Composites-Advances in Ceramic Armor*, in press (2006)
[4] J.M. Wells, Progress in the Nondestructive Analysis of Impact Damage in TiB_2 Armor Ceramics, *Proceedings of the 30th International Conference on Advanced Ceramics and Composites-Advances in Ceramic Armor*, in press (2006)
[5] J. M. Wells, Progress on the NDE Characterization of Impact Damage in Armor Materials, *Proceedings of the 22nd International Ballistics Symposium*, Adelaide, Au, ADPA, **2**, 793-800 (2005)
[6] H.T. Miller, W.H. Green, N. L. Rupert, J.M. Wells, Quantitative Evaluation of Damage and Residual Penetrator Material in Impacted TiB_2 Targets Using X-Ray Computed Tomography, *21st International Symposium on Ballistics*, Adelaide, Au, ADPA, **1**, 153-159 (2004)
[7] J.M. Wells, W.H. Green, N.L. Rupert, J. R. Wheeler, S.J. Cimpoeru, A.V. Zibarov, Ballistic Damage Visualization and Quantification in Monolithic Ti-6Al-4V with X-ray Computed Tomography, *21st International Symposium on Ballistics*, DSTO, Adelaide, Au, ADPA, **1**, 125-131 (2004)
[8] J. R. Wheeler, W. H. Green, M. Schuresko, M.P. Lowery, A Framework for the Analysis and Visualization of X-ray Computed Tomography Image Data Using a Computer Cluster, *Proceedings of 22nd International Symposium on Ballistics*, **1**, 569-576 (2005)
[9] Dennis, M.J., *Nondestructive Evaluation and Quality Control*, Industrial Computed Tomography, ASM Handbook, American Society for Metals International, **17** (1989)